Investigating the efficiency of aeroplane winglets using FEM

Anuj Baskota[1]

[1]Department of Biological Engineering, Cornell University
Ithaca, NY 14850, USA

Abstract. *Strategic design of aircraft wings have evolved over time for maximum fuel efficiency. One of such ideas involves winglet which has been known to reduce turbulence at the tip of the wings. This study intends to investigate the differences in drag and lift forces generated at aeroplane wings with and without winglet at cruising speed using FEM. Simulations were performed in the SST turbulence model of CFD and the results are compared to that of the experimental and theoretical models. The simulation showed that the lift increased by* 26.0% *and the drag decreased by* 74.6% *for the winglet at cruising speed.*

1. Introduction and theory

Wings are one of the fundamental units which allow airplanes to fly. The basic concept of flight is usually derived from Bernoulli's equation which is stated as the pressure of a fluid decreasing when its velocity increases, provided that the potential energy is constant. When an airplane moves at a high speed, the air flowing over the top of the wings decreases the air pressure. This makes the air pressure at the top of the wings lower than that of the bottom. The net pressure generates a lift force, which is in the upward direction, makes the wing move upwards, thus allowing the airplane to fly.

Bernoulli's equation:

$$\frac{1}{2}\rho v_1^2 + mgh_1 + P_1 = \frac{1}{2}\rho v_2^2 + mgh_2 + P_2 \tag{1}$$

Here, potential energy can be ignored as $h2 - h1 = 0$

$$P_2 - P_1 = \frac{1}{2}\rho(v_1^2 - v_2^2) \tag{2}$$

Here, $P_2 - P_1$, the net pressure is positive as $v_1 > v_2$ Overall for the aircraft to move upwards, the force generated by this pressure difference must be greater than the gravitational force of the wing which is acting downwards.

In airplanes, forces like lift and thrust provided by the engine help move airplanes in the upward and forward direction respectively. Similarly, resistance forces such as drag act in the opposite direction to the relative motion between the object and the fluid. This drag force generated at the wings depends on the effective area of the wing facing the airflow and the shape of the aerofoil. During the time of flight, the airflow over the tip of the wing is forced back causing the air to curl around it in an upward direction forming a vortex. These vortices cause lift-induced drag which can be strong enough to flip an entire aircraft. This drag also causes energy loss in the wings.

The total drag of an aeroplane wing can be quantified by the following equation:

$$C_d = C_{do} + C_{di} \tag{3}$$

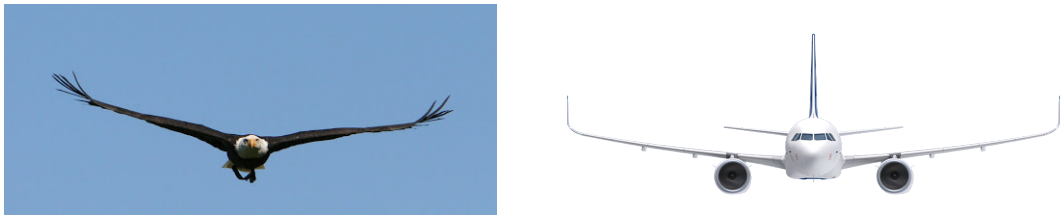

(a) An Eagle (b) Airbus 320 Neo

Figure 1. Bio-inspired winglet similarities between an eagle and A320 Neo.

where C_d is the total drag coefficient, C_{do} is the base drag which occurs at zero lift, and C_{di} is the induced drag.

One of the strategies implemented in order to minimize the effect of drag in the airplane wings is having winglets [MTU(2018)]. Winglets are the curved shape of the tip of the airplane wings. The bent shape of the wings provides a forward lift which opposes the drag produced by the vortices. Thus overall, winglets favor the forward motion of the airplane which results in fuel efficiency. According to the flight test conducted in NASA Dryden Flight Research Center, the fuel use of Boeing 707 airliners with winglets resulted in a 6.5% reduction compared to the regular rectangular wingtip [NASA(2008)]. The design of winglets in airplanes is usually known to be bio-inspired mimicking the gliding of eagles, hawks, or other birds of prey as shown in Figure 1 [Tucker(1995)].

This project intends to compare wings with regular tips to the wings with winglets to analyze the lift and drag coefficients during a flight using Computational Fluid Dynamics (CFD). COMSOL Multiphysics was used to run the simulations. Here, wings at 0 angle of attack at cruising speed were modelled.

2. Method and Use of COMSOL Multiphysics® Software

2.1. Domain selection

The airplane wings both with and without winglets were designed using AutoDesk Inventor and converted into an .stl file which was then imported into COMSOL. These designs represent simplified model of an average commercial aircraft wings. The wings dimension was approximately $17.5m$ length, $6.8m$ maximum width, and maximum airfoil thickness was $0.8m$. The winglet adds an extra $1m$ in length and $2m$ in height. In this simulation, the computation domain however, is the air surrounding the wings. Therefore, the wings were placed inside a cuboid which represents the air domain of dimension 20m x 10m x 5m. This volume was selected so that it is enough to capture the major changes in the fluid flow at the structure/fluid boundary but small enough to have a relatively fast model in terms of computation time and storage.

2.2. Governing Equation

COMSOL's built-in fluid module uses Navier-Stokes equations as shown in 4). The SST model combines the near-wall capabilities of the kω model with the superior free-stream behavior of the k ϵ model to enable accurate simulations of a wide variety of internal and external flow problems. This model's equation is based on k and ω , where ω is the specific dissipation rate.

$$\frac{\partial(\rho\overrightarrow{u})}{\partial t} + \overrightarrow{\nabla} \cdot (\rho\overrightarrow{u}) = -\overrightarrow{\nabla p} + \overrightarrow{\nabla} \cdot \overline{\overline{\tau}} + \rho\overrightarrow{f} \tag{4}$$

where ρ is the density of air, u is the velocity, p is the pressure, τ is the tensile stress, and f is the external force which in our case is gravity.

2.3. Boundary Conditions

The front side fluid domain was considered to be an inlet with the speed of $250m/s(560mph)$ which corresponds to a general cruising velocity of airplanes. The back side was set to be the outlet with $0Pa$ pressure. The remaining 4 sides were assigned as symmetry boundary condition which represents the open boundaries.

2.4. Mesh Generation

Free tetrahedral mesh was generated with 260,530 domain elements in fluid domain as shown in Figure 3. This was the predefined fine setting in COMSOL. The elements of this mesh was calibrated for general physics. In addition, distributed mesh was used around the winglet/fluid boundary in order to capture minor changes of velocity and pressure around this region. The boundary element number was 18,324 where as the edge element was 1884.

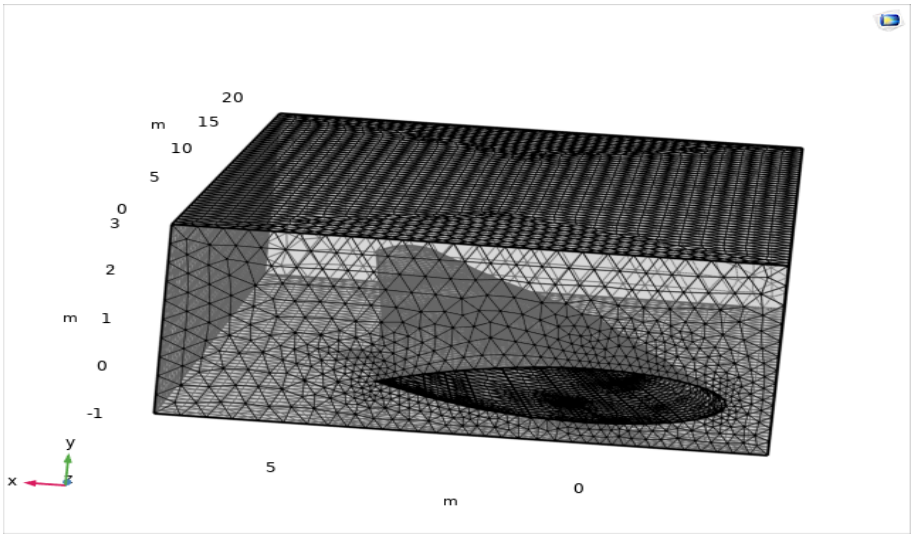

Figure 2. Mesh of the fluid domain and the winglets

2.5. Lift and Drag Force Derivation

For this particular simulation, the goal was to compare whether the airplane wing is more efficient with a winglet. As mentioned in the introduction, the flight can be more efficient with minimum resisting forces and maximum driving forces. Therefore, the force components of drag and lift generated in the wings provide a better understanding on the overall resistance of the aircraft. Coefficient of drag and lift were calculated to compare the efficiency of the wings. The lift (L) and drag (D) forces are as follows [NASA(2014)]:

$$L = \frac{1}{2} C_L \rho S u^2 \tag{5}$$

$$D = \frac{1}{2} C_D \rho A u^2 \tag{6}$$

where u is the velocity of fluid, ρ is the density, C_L and C_D are coefficients of lift and drag respectively. The area that is considered while calculating lift and drag are different. Here, A is the area of the wings which come in contact with the inlet fluid (parallel to the drag) and S is the area of the wings (perpendicular to the lift) which is perpendicular to the lift force.

In COMSOL, these forces were derived using specific expressions for fluid flow without wall function. **Table 1** shows the expressions that will be integrated in either x,y, or z directions depending on the direction of the force.

Table1: Expressions used for components of drag and lift forces.

Force expressions		
	Drag	Lift
Pressure Force	$spf.nxmesh * p$	$spf.nymesh * p$
Viscous Force	$-spf.K_stressx$	$spf.nymesh * p$
Total Force	$-spf.T_stressx$	$spf.nymesh * p$

2.6. Computation Details

The analysis was performed as a steady state fluid flow. The Iterative solver (GMRES) was used to run the stationary simulations in COMSOL. The absolute tolerance was set as 0.1. The average computation time for one simulation was approximately 40 minutes.

3. Results and Discussion

To analyze the effect of airflow on the wings, graphics of static pressure at the steady-state was extracted. This is the 3-D pressure field plot of the wings. This allowed us to visualize the pressure distribution throughout the wings and also compare the pressure values between the winglet and no winglet configuration. The pressure experienced by the wings is least at the center as observed in Figure 3 and Figure 4. We can also observe increasing pressure at the edge of the wings where the air leaves the wings. In realistic scenarios, the pressure at this edge would be less due to the curved airfoil. From Figure 3 and Figure 4, we see that the magnitude of pressure at the front-facing side of the wing is less with winglet configuration. The pressure is distributed along the edge of the winglet which helps the airplane wings to be more steady. Similarly, we observe increasing pressure in the outer edge of the winglet which would also contribute to increasing lift along the z-axis. This provides extra lateral stability of the wings as well as contribute to the overall lift.

To compare the efficiency, drag and lift forces were calculated using the method provided above from COMSOL. Table 2 shows the force components of drag and lifts for the winglet and no winglet configulations. The coefficient of lifts and drag were calculated using the equations 5 and 6 and the values are provided in Table 3. Here, the winglet had an increase in the lift force by 26.0% and decrease in the drag by 74.6%. The ratio of lift to drag was 10.2 and 2.04 for the winglet and no winglet configurations. In realistic cases, the Boeing 747-4 and the Airbus A330-300 have lift to drag ratio of 15.5 and 18.1 [Rodrigo Martínez-Val(2005)].

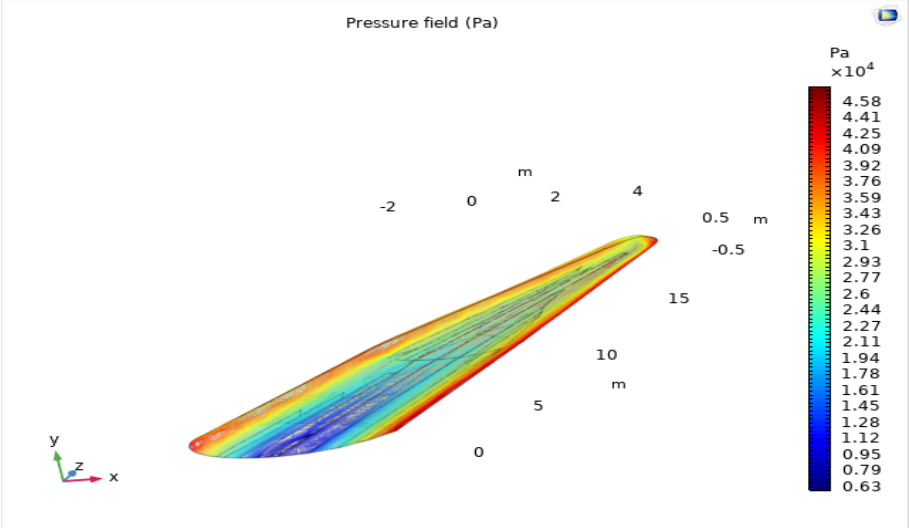

Figure 3. Static pressure observed at steady state for no winglet configuration.

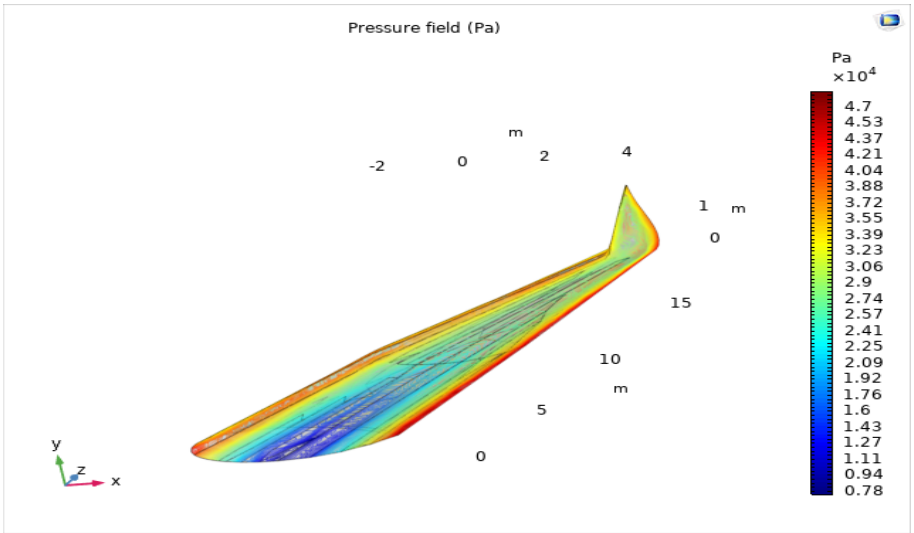

Figure 4. Static pressure observed at steady state for winglet configuration.

Table2: Components of lift and drag forces generated.

Force components (N)				
	Force	Pressure (-)	Viscosity	Total (-)
Winglets	Lift	$3.541e5$	48.001	$3.54e5$
	Drag	$3.489e4$	39.778	$3.485e4$
No Winglets	Lift	$2.8087e5$	25.577	$2.8085e5$
	Drag	$2.925e4$	41.589	$2.922e4$

Usually at high speed, the Reynolds number is very high. However, in the boundary layer that is very close to the wall of the wings, the velocity is lower due to which the viscous force has a higher effect [NASA(2015)]. In our case, the obtained viscous forces are very small compared to the force due to the pressure. Viscous forces, although low in magnitude, might cause severe drag in boundary layers where the velocity (inertia effect) is minimum. In our simulation, we obtained lower viscous forces in both cases which

helps to reduce the drag along the wings.

Table3: Coefficients of lift and drag.

Coefficient of total force		
	Lift	Drag
Winglets	$1.46E-01$	$1.44E-02$
No Winglets	$1.16E-01$	$5.68E-02$

4. Conclusion

The results obtained from this simulation concludes that for wings at 0 angle of attack, presence of winglets reduce the drag by 74.6% and increase the lift 26.0% when cruising. The pressure at the front side of the wing is more distributed with winglet presence which also helps to stabilize the wings. Similarly, it was also observed that there is an extra component of force generated at the winglet which contributes to the lift of the whole aircraft making it more efficient. Thus, the results showed that the winglets make the airplane wings more efficient. Simulations with varying angle of attack, cant angles, cruising speed, and other physical features can be performed to further understand the efficient flight of an aeroplane.

References

MTU. How winglets work. *AeroReport*, 2018.

NASA. Winglets. *Dryden Flight Research Center*, 2008.

Vance A Tucker. Drag reduction by wing tip slots in a gliding harris' hawk, parabuteo unicinctus. *Journal of experimental biology*, 198(3):775–781, 1995.

NASA. Modern drag equation. *Glenn Research Center*, 2014.

Jose F. Palacin Rodrigo Martínez-Val, E. O. Pérez. Historical evolution of air transport productivity and efficiency. *43rd AIAA Aerospace Sciences Meeting and Exhibit*, 2005.

NASA. Boundary layer. *Glenn Research Center*, 2015.